DOI: 10.1111/j.1751-1097.2008.00312.x

The Length of Esterifying Alcohol Affects the Aggregation Properties of Chlorosomal Bacteriochlorophylls

Anita Zupcanova[1,2], Juan B. Arellano[3], David Bina[1,4], Jiri Kopecky[2,5], Jakub Psencik[*,2,6] and Frantisek Vacha[1,2]

[1] Biological Centre, Academy of Sciences of the Czech Republic, Branisovska 31, 370 05 Ceske Budejovice, Czech Republic.

[2] Institute of Physical Biology, University of South Bohemia, Zamek 136, 373 33 Nove Hrady, Czech Republic.

[3] Instituto de Recursos Naturales y Agrobiología (IRNASA-CSIC), Apdo. 257, 37071 Salamanca, Spain.

[4] Faculty of Science, University of South Bohemia, Branisovska 31, 370 05 Ceske Budejovice, Czech Republic

[5] Institute of Microbiology, Academy of Sciences of the Czech Republic, Opatovicky mlyn, 379 81 Trebon, Czech Republic

[6] Faculty of Mathematics and Physics, Charles University, Ke Karlovu 3, 121 16 Prague, Czech Republic.

[*]Corresponding author email: psencik@karlov.mff.cuni.cz (Jakub Psencik)

ABSTRACT

Chlorosomes, the main light harvesting complexes of green photosynthetic bacteria, contain bacteriochlorophyll (BChl) molecules in the form of self-assembling aggregates. To study the role of esterifying alcohols in BChl aggregation we have prepared a series of bacteriochlorophyllide *c* (BChlide *c*) derivatives differing in the length of the esterifying alcohol (C_1, C_4, C_8 and C_{12}). Their aggregation behavior was studied both in polar (aqueous buffer) and non-polar (hexane) environments and the esterifying alcohols were found to play an essential role. In aqueous buffer, hydrophobic interactions among esterifying alcohols drive BChlide *c* derivatives with longer chains into the formation of dimers, while this interaction is weak for BChlides with shorter esterifying alcohols and they remain mainly as monomers. All studied BChlide *c* derivatives form aggregates in hexane, but the process slows down with longer esterifying alcohol due to competing hydrophobic interactions with hexane molecules. In addition, the effect of the length of the solvent molecules (*n*-alkanes) was explored for BChl *c* aggregation. With an increasing length of *n*-alkane molecule, the hydrophobic interaction with the farnesyl chain becomes stronger, leading to a slower aggregation rate. The results show that the hydrophobic interaction is the driving force for the aggregation in aqueous environment, while in non-polar solvents it is the hydrophilic interaction.

INTRODUCTION

The main light-harvesting complexes of green photosynthetic bacteria are called chlorosomes. They form ellipsoidal bodies attached to the inner side of the bacterial cytoplasmic membrane (1). In contrast to all other photosynthetic complexes, chlorosomes contain large amounts of self-assembling bacteriochlorophyll (BChl) *c*, *d* or *e* aggregates (2). In these aggregates, BChl molecules are held together by intermolecular coordination of the central Mg ion of one BChl molecule to the hydroxyethyl at $C3^1$ of a second BChl. An additional interaction found in BChl aggregates is now a matter of debate and two models have been put forward to explain it. In the first model a hydrogen bond is formed between the hydroxyethyl at $C3^1$ of the second BChl and the keto group at $C13^1$ of a third BChl molecule (3). The second model proposes that the keto group at $C13^1$ of the second BChl is weakly coordinated to the central Mg ion of yet another BChl (4). These intermolecular interactions between the polar heads of chlorosomal BChl molecules are responsible for the arrangement of the building blocks of the BChl aggregates. However, the nature of the building block is not yet clear and the existing structural models for BChl aggregates can be divided into two groups based on asymmetric repeating unit. In the first group, BChl aggregates are suggested to form parallel-chains with BChl monomer as the building block (5-8). In the second group BChl aggregates are proposed to consist of antiparallel BChl dimers as the smallest repeating unit (9-14). The terms parallel and antiparallel refer here to the mutual orientation of the Q_y transition dipoles of BChl molecules. Another question arises concerning how the BChl aggregates are arranged at long-range order inside chlorosomes. According to original models, BChl aggregates form hexagonally packed rod-like structures of 5 or 10 nm diameter (5,8,14-16). Recently, a new model of BChl

organization was proposed, in which undulated planes of BChl aggregates are interdigitated into lamellar structures (17,18). The X-ray diffraction data support the dimer as the building block of the aggregate (17). The lamellar nature of the BChl aggregates was confirmed in a very recent electron cryomicroscopy study (19), which provides an improved insight into long-range organization of BChl *c* aggregates in *Chlorobium tepidum.*

Artificial BChl aggregates with very similar optical properties to chlorosomes can be prepared also *in vitro* either in non-polar solvents or in aqueous buffers with addition of lipids, detergents or carotenoids (20-23). Self-aggregation was also reported for synthetic chlorins with the hydroxy and keto groups located along the Q_y axis of the chlorin derivative and with coordinated central metal ion (24,25), however, it is also possible to use other recognition groups for the formation of synthetic BChl aggregate mimics (26). The extensive research on BChl aggregates and artificial self-assembling porphyrins is reviewed in (1,2,4,27-29).

The role of esterifying alcohols has been summarized in a recent review (30). In most photosynthetic antennae an interaction between (B)Chl molecules and the protein scaffold exits. In these complexes the esterifying alcohols play an essential role in anchoring the (B)Chl molecule to the antenna by molecular interactions with hydrophobic domains of the protein skeleton (31-33). In chlorosomes, the aggregates are formed with no assistance of protein and the esterifying alcohol of BChls can be modified without changing significantly the spectral properties of chlorosomes. This was shown by incorporation up to 60% of externally added alcohols (with a carbon skeleton of C_{10}-C_{20}) into BChls of *Chlorobium tepidum* and *Chloroflexus aurantiacus* (34,35) Only addition of dodecanol to *Chlorobium tepidum* culture caused observable blue shift (6 nm) of the Q_y band of BChl *c* in chlorosomes. Furthermore, changes in the

Formatted: Formatted

Deleted: 19 Deleted: 2 Deleted: 1 Deleted: 3 Deleted: 4 Deleted: 5 Deleted: 6 Deleted: 8 Deleted: 29 Deleted: 0 Deleted: 2 Deleted: 3 Deleted: 4

Q_y band position of BChl *c* aggregates have been investigated upon the exchange of the esterifying alcohol from farnesyl to hexyl, propyl and methyl (30). Whereas no changes for 3^1-epimeric mixture of the C8 and C12 homologues have been observed in non-polar organic solvents, a 10-nm red shift was induced in aqueous Triton X-100 solutions. The red shift was less pronounced if the exchange of the farnesyl group for shorter alkyl groups was investigated with pure 3^1-R BChl *c* having ethyl groups at C8 and C12 (36)

The hydrophobic interaction between the farnesyl chain and lipids (22) or carotenoids (23) has been shown to be strong enough to drive the formation of BChl *c* aggregates in aqueous buffer, while bacteriochlorophyllide *c* without any esterifying alcohol (H-BChlide *c*) was not able to form aggregates under any circumstances (23). This suggests that the length of the esterifying alcohol might be crucial for the aggregation ability. In this work we explore aggregate formation by synthetic X-BChlide *c* derivatives varying in the length of their *n*-alkyl chain both in polar (aqueous buffer) and non-polar (hexane and other *n*-alkanes) environments. Due to excitonic coupling between pigments, absorption spectroscopy is a sensitive technique to monitor the degree of aggregation. Our results demonstrate that the length of the esterifying alcohol plays an essential role in the build-up of BChl aggregates. Further, it is shown that the driving force for the aggregation is the hydrophobic interaction (between esterifying alcohols) in aqueous environment and the hydrophilic interaction (between chlorin rings) in non-polar solvents.

Deleted: 29

Deleted: 1

Deleted: 2

Deleted: 2

MATERIALS AND METHODS

Growth conditions of Chlorobium tepidum and isolation of BChl c. Cells of the green

sulfur bacterium *Chlorobium tepidum* were cultured in 800 ml of modified Pfenning's medium (37) for 3 days at 48°C in 1-liter flasks in water bath under constant illumination from a 60 W Tungsten lamp (100–200 µmol m^{-2} s^{-1} at the water surface of the bath). BChl *c* was extracted from the cell culture by means of a mixture of acetone and MeOH (7:2, vol/vol) and further purified by reverse HPLC as described in (23). The four main C8 and C12 homologues of BChl *c* (*i.e.* [E,M]BChl *c*, [E,E]BChl *c,* [P,E]BChl *c,* [I,E]BChl *c*, where E, M, P and I stand for ethyl, methyl, propyl and isobutyl, respectively) containing esterified farnesyl at the C17 propionic acid side chain (*i.e.* $C17^3$) were pooled together, dried and kept under inert atmosphere at –20 ºC until use.

Deleted: 5

Deleted: methanol

Deleted: 2

X-Bacteriochlorophyllide c derivatives preparation and MS analysis. X-Bacteriochlorophyllide *c* (X-BChlide *c*) derivatives, where X stands for methyl (Me), butyl (Bu), octyl (Oc) and dodecyl (Do) at the $C17^3$ position, were prepared from BChl *c* by transesterification under KOH alkaline conditions. Except for Do-BChlide *c*, all X-BChlide *c* derivatives were prepared directly from BChl *c* as follows. An amount of 60 nmoles of dried BChl *c* was dissolved in 150 µL of a reaction mixture containing KOH dissolved in the appropriate *n*-alcohol (X-OH). Several KOH concentrations were used, but the optimal one was determined to be about 0.1% (w/vol), for which the amount of remaining BChl *c* (dominating at lower KOH concentrations) and accumulated H-BChlide *c* (dominating at higher KOH concentrations) was minimal. The mixture containing BChl *c* was incubated in dark for 30 min at 30°C in a water bath. After the treatment, X-BChlide *c* derivatives were separated from H-BChlide *c* or remaining BChl *c* by high performance liquid chromatography (HPLC) in a semi-preparative SGX C-18 reverse phase column (7 µm, 8×250 mm, Tessek, Czech Republic) using a Waters

HPLC system consisting of Pump Controller 600, Delta 600 injection system and a PDA 996 detector (Waters, USA). The HPLC was performed at room temperature using an isocratic elution with 100% HPLC grade MeOH at a flow rate of 2 mL min^{-1}. Since the retention time of Do-BChlide *c* is close to the one of BChl *c* and their peaks partially overlap (see Results and Fig. 1), the Do-BChlide *c* was prepared from Me-BChlide *c* using the same procedure as described above. The four main C8 and C12 homologues of all X-BChlide *c* derivatives were collected in one single pool. The HPLC-purified X-BChlide *c* derivatives were dried thoroughly under a stream of nitrogen. Traces of amphiphilic contaminants (*i.e*. free X-OH) that could accompany the X-BChlide *c* derivatives were washed out by means of hexane. After several washes of dry pigments with an excess of hexane, the remaining hexane was blown out with a stream of nitrogen and the dried X-BChlide *c* derivatives were kept under inert atmosphere at -20°C until use.

Mass spectrometry (MS) analysis of the prepared X-BChlides was performed on a HPLC Agilent 1100 with a MSD SL-Ion Trap mass spectrometer and electrospray ion source (Agilent Technologies, USA). The ion trap mass spectrometer was optimized for ions with *m/z* (mass-to-charge) ratio 600 in a positive mode. The spray needle was at a potential of 4.5 kV, and a nitrogen sheet gas flow of 20 (a.u.) was used to stabilize the spray. The counter electrode was heated to 200°C, and the stainless-steel capillary held at a potential of 10 V. The tube-lens offset was 20 V, and the electron multiplier voltage was -800 V. Helium gas was introduced into the ion trap at a pressure of 0.13 Pa to improve the trapping efficiency of the sample ions introduced into the ion trap. The background helium gas also served as the collision gas during the collision activation dissociation. A typical experimental protocol for the direct infusion MS/MS experiments consisted of injection a solution of purified chlorophyll derivatives in

100% MeOH with 0.1% formic acid into the ion-trap mass spectrometer via a 250-µL syringe at a flow rate of 50 µL min^{-1}.

Deleted: methanol

Pigment aggregates. Aggregates of BChl *c* or X-BChlide *c* derivatives were prepared both in aqueous buffer and in non-polar solvents. In the first case, dried BChl *c* or X-BChlide *c* derivative was dissolved in MeOH. A volume of 10 µl of the resulting mixture was slowly injected into vigorously vortexed 3 ml of buffer (50 mM Tris-HCl, pH 8.0). In the second case, the same procedure was followed except that BChl *c* or X-BChlide *c* derivative was dissolved in 10 µl HPLC grade dichloromethane and injected into vigorously vortexed 3 ml of HPLC grade hexane or other *n*-alkanes. In both cases, the final concentration of pigments was approximately 20 µM. BChl *c* forms a mixture of monomers and dimers in dichlormethane at the used concentrations. When the effect of lipids on the aggregation was studied, monogalactosyl diglyceride (MGDG, Sigma, USA) was added to the MeOH-dissolved pigments prior to injection into the aqueous buffer. The maximal final concentration of MGDG was 40 µM. Experiments with aggregates were performed at room temperature (26±2°C).

Absorption spectra. Absorption spectra were measured using Spectronic Unicam UV-300 spectrophotometer (Cambridge, UK) in 1-cm path glass cuvettes. Spectra were normalized to a constant area under the spectrum (when plotted with an x-axis in energy units). The normalization is based on the assumption that the overall oscillator strength of pigment molecules in different aggregation states must be conserved; and that the length of the esterifying alcohol does not alter the oscillator strength of the pigment.

RESULTS

To better understand the role of the esterifying alcohol in aggregation of chlorosomal BChls, we have prepared a set of X-BChlide derivatives differing in the length of the esterifying alcohol at C17[3]. We have chosen the length of the *n*-alcohol chain to be 1 (Me-BChlide *c*), 4 (Bu-BChlide *c*), 8 (Oc-BChlide *c*) and 12 (Do-BChlide *c*) carbons. The range of selected X-BChlide derivatives is limited by the fact that the respective alcohols must be liquid at 30ºC and dissolve KOH at least up to 0.1% (w/vol) at this temperature. Transesterification of BChl *c* was originally reported to prepare Me-BChlide *c* at room temperature using anhydrous potassium carbonate (6). Several suitable Lewis bases such as alkali carbonate, hydroxide, or alkoxide, or an organic amine can be used for transesterification reactions. Potassium carbonate has the advantage that the reaction yield is high and it can be decomposed to carbon dioxide and carbon dioxide removed by vacuum; however, it has the disadvantage that it cannot be dissolved in some of the alcohols we have made use of. In this respect, KOH was found a very suitable catalyst and chemical transesterification of BChl *c* could be performed efficiently without high degradation of BChl *c*. Me-BChlide *c* is the shortest X-BChlide *c* derivative in this study and is used instead of H-BChlide *c* to avoid the ionic nature of the non-esterified propionic acid side chain at C17. The length of dodecyl carbon skeleton corresponds to the length of farnesyl (without methyl side-chains), which is the main esterifying alcohol for *Chlorobium tepidum*. The time course of X-BChlide aggregate formation was monitored during the first 24 hours.

Formatted

Deleted: Under these conditions,

Deleted: can

HPLC purification and MS identification of X-BChlide *c* derivatives

Figure 1 shows HPLC chromatograms of individual X-BChlide *c* derivatives detected at 430 nm. The HPLC peaks with retention time between 9 and 11 min were identified as the main four homologues of BChl *c* (i.e. [E,M], [E,E], [P,E] and [I,E], see also MS results below) and the molar ratio between them was determined to be <1:61:33:5. This molar ratio is in agreement with the expected degree of alkylation of C8 and C12 at high-light irradiance (>50 µmol m^{-2} s^{-1})(38). Chromatograms were normalized to a constant area under the curve. This normalization is based on the assumption that all X-BChlide *c* derivatives have the same extinction coefficient in MeOH. HPLC chromatograms are presented to illustrate changes in polarity between different X-BChlide derivatives and BChl *c*. To show the ability of the chromatography procedure to separate individual X-BChlide derivatives, Fig. 1c–f shows HPLC chromatograms obtained at lower KOH concentrations (<0.1% in the reaction mixture), where peaks ascribed to both X-BChlide *c* derivatives and remaining BChl *c* appear simultaneously. Figure 1f shows the HPLC chromatogram of Do-BChlide *c* for which Me-BChlide *c* was used as the starting reactant. Retention times were between 5–6 min for Me-BChlide *c*, 6–7 min for Bu-BChlide *c*, 7–9 min for Oc-BChlide *c* and 10–12 min for Do-BChlide *c*. The retention time of H-BChlide *c* was around 3 min. The observed retention times corresponded well with the expected polarity of each X-BChlide *c* derivative. It is worth noting that the four peaks of the main pigment homologues are not completely resolved due to the selection of an isocratic elution run with 100% MeOH. The resolution of the HPLC chromatograms at early times could be improved when the initial mobile phase contains H_2O and a linear gradient is used between H_2O:MeOH (1:9, vol/vol) and pure MeOH. However, the presence of water in the

Deleted: 6

collected fractions of X-BChlide *c* derivatives delays pigment drying and undesirably drives pigments to degradation. The procedure used in this work allowed to separate pigments and dried them in an optimal way. The HPLC profile was dominated by a large contribution of the [E,E] and [P,E] homologues, which together accounted for more than 90% of the total amount of the four homologues. The first ([E, M]) and last ([I, E]) homologues were present in very small amounts. Nevertheless, experiments were performed with this naturally occurring mixture of the four main homologues found under our cell growth conditions.

Further confirmation of the pigment identity was performed by means of MS. The results summarized in Table 1 show the agreement between the experimental and theoretical molecular masses of the four main homologues of BChl *c* and the homologues of the prepared X-BChlide *c* derivatives. Because of the small amounts of [E, M] and [I, E] homologues, their presence could not be detected in many cases by mass spectrometry (Table 1). Absorption spectra of all studied X-BChlide derivatives in MeOH were undistinguishable from spectra of BChl *c* (not shown). These facts confirm identification of the prepared X-BChlides.

Absorption spectra of X-BChlide *c* derivatives in aqueous buffer

The effect of esterifying alcohol length on X-BChlide *c* aggregation in aqueous buffer is illustrated in Fig. 2. Me-BChlide *c* has the shortest tail and therefore it is a polar molecule. As a result, it is well soluble in aqueous buffers and quickly after preparation (<5 min) the absorption spectrum reaches the steady state where the prevailing form is a monomer with a maximum at 676 nm (Fig. 2a and inset). On increasing the esterifying alcohol length of the X-BChlide *c* derivatives, a concomitant increase in absorbance at

around 710 nm is observed together with a slower evolution of the spectral properties (Fig. 2b–d). The absorption spectrum of Do-BChlide *c* exhibits the slowest evolution. While the monomeric form is prevailing also for Do-BChlide *c* 5 min after preparation (Fig. 2, inset), the 710 nm band is clearly discernible after 24 hours (Fig. 2d). The results shows that the increase in the non-polar character of the X-BChlide *c* derivatives leads to a development of another spectral form of X-BChlide *c* derivatives, which is induced by more intense hydrophobic interaction between the molecules in aqueous buffer. The presence of methyl substituents and double bonds in the farnesyl group of BChl *c* promotes better formation of the absorption band at 710 nm than the dodecyl group of Do-BChlide *c*, which has the same skeleton length (C_{12}) as farnesyl (Fig. 2e). The BChl *c* form with a main Q_y maximum at 710 nm has been previously attributed by NMR to a mixture of antiparallel and T-shaped dimers of BChl *c* in organic solvents (3). Later, the BChl *c* form with basically identical spectrum was also observed in aqueous buffer (2). We will denote this species as 'dimers' in this work to distinguish them from higher-state aggregates. It should be stressed that the presented absorption spectra of X-BChlide *c* derivatives were obtained without use of lipids, detergents or any other additions. No aggregates in higher state than dimers were observed even after several days of incubation.

It is known that BChl *c* forms (higher-state) aggregates in aqueous buffer in the presence of lipids, e.g. MGDG (1,2,2,2,6). We have observed similar aggregates also when using the X-BChlide derivatives. All studied X-BChlides formed aggregates in the presence of MGDG, however, a slight decrease in the rate of aggregate formation with an increase of the polar character (*i.e.* with shorter esterifying alcohol) was discernible. Nevertheless, already after 4 hours all the X-BChlide *c* derivatives formed structures with very similar absorption spectra to BChl *c* aggregates (data not shown).

Deleted: radical
Deleted: radical
Deleted: 7
Deleted: 2
Deleted: 1
Deleted: 5

Absorption spectra of X-BChlide *c* derivatives in hexane

The BChl *c* aggregates can be formed not only in aqueous environment when lipids or carotenoids are present, but also in various non-polar organic solvents. In the latter case, pure BChl *c* forms aggregates with no further additions. Apparently, the driving force for aggregation in non-polar solvents is the hydrophilic interaction between the polar chlorin heads rather than the hydrophobic interaction between esterifying alcohols. Therefore it is interesting to investigate whether the length of esterifying alcohol also affects the aggregation of X-BChlide *c* in non-polar solvents. In this work we used hexane. Figure 3 brings together the absorption spectra of X-BChlide *c* derivatives and BChl *c* in hexane after 4 hours of incubation. They all form aggregates and the absorption spectrum of every X-BChlide *c* derivative resembles that of BChl *c* aggregates in hexane (with the main Q_y maxima around 745 nm). An increase in the rate of aggregate formation with an increase of the polar character (*i.e.* with shorter esterifying alcohol) was discernible. However, not every X-BChlide *c* molecule is incorporated in the aggregate. A close inspection of the absorption spectra of X-BChlide *c* derivatives reveals that, when increasing the length of the *n*-alkyl substituent, the absorption bands at 635, 675 and 710 nm, typical for BChl *c* dimers (see also Fig. 4), become more apparent (2,3,9). In addition, the increase in absorbance at 675 nm is more prominent than at 635 and 710 nm, which indicates presence of residual monomers. It can be seen that the amount of monomers and dimers increases with the length of the esterifying alcohol. The absorption bands at 635, 675 and 710 nm are also observed in pure BChl *c*, although they are less prominent compared to Do-BChlide *c*. This suggests again that the methyl substituents and the double bonds in the skeleton of

Deleted: 2

Deleted: 7

farnesyl improve the aggregation BChl *c*.

As already mentioned, the aggregate formation was slower for X-BChlides with longer esterifying alcohols. The inset of Fig. 3 shows that Do-BChlide *c* forms a significant portion of dimers shortly after preparation, which later converted into aggregates. On the other hand, absorption spectra of Me-BChlide *c*, which is a rather polar molecule, are characterized by a dominant contribution of higher-state aggregates already immediately after preparation. It can be noted that the aggregation of all X-BChlide *c* derivatives leads few hours after preparation to formation of macroscopic flaked-like aggregates that precipitate in the cuvette, similarly as reported for BChl *c* (40).

Deleted: 38

BChl *c* in *n*-alkanes

As shown above, the aggregation rate in hexane is slower for X-BChlide *c* derivatives with longer esterifying alcohol. This indicates that the rate of aggregate formation in non-polar solvents is hindered by the hydrophobic interaction of the esterifying alcohol with the solvent. This observation has led us to investigate aggregation of BChl *c* in a series of *n*-alkanes with a different molecule length: hexane, octane, decane, dodecane and tetradecane. All of them are liquid at room temperature. Figure 4 shows absorption spectra of BChl *c* dissolved in these *n*-alkanes after 24 h incubation. It is well known that BChl *c* in hexane forms aggregates readily (see also Fig. 3), however, we observed that, on increasing the length of solvent molecules, BChl *c* aggregates are formed less efficiently and more slowly as revealed by higher amount of dimers in absorption spectra (Fig. 4). The changes in absorption spectra of BChl *c* suggest that the hydrophobic interaction of farnesyl tail is stronger with longer *n*-alkanes, which

opposes the aggregate formation. For the tetradecane, as the longest *n*-alkane solvent, BChl *c* forms mainly dimers during the first 15 min after preparation, which later evolves to a mixture of dimers and higher-state aggregates (Fig. 4, inset). On the same time scale (15 min), BChl *c* aggregates were already dominant in hexane.

Due to slower aggregation, it is clearly visible the formation of BChl *c* dimers as an intermediated state before development of aggregates in non-polar solvents. The slight differences in band-widths and positions of absorption maxima of dimers in *n*-alkanes and aqueous buffer are caused by solvent shift, however, the spectra retain the same characteristic profile. An illustration of the time course of the aggregation is given in Fig. 5 where absorption spectra of BChl *c* in decane were monitored during 48 hours after preparation. An isosbestic point arising from conversion of the dimers (absorption maxima at 635, 675 and 710 nm) to aggregates (absorption maximum at 750 nm) is observed near 720 nm.

DISCUSSION

A series of X-BChlide *c* derivatives has been chemically synthesized to investigate the effect of esterifying alcohol on the aggregation of chlorosomal BChls. The four main homologues of BChl *c* (and all the prepared X-BChlides) were used in the same ratio as they are naturally found in chlorosomes. The natural mixture of the four C8 and C12 homologues (together with the $C3^1$ diasteroselectivity) of BChl *c* produces aggregates with spectral properties very similar to the BChl *c* aggregates in chlorosomes. In contrast, individual C8 and 12 homologues or separated 3^1-R and 3^1-S epimers produce aggregates with spectral properties that depend remarkably on the degree of alkylation in C8 and C12 or in the selected $C3^1$ diasteroisomer (4,41-44). All this gives good

Deleted: 39

Deleted: 2

Deleted: .

reason for the use of the naturally occurring mixture of the homologues in this study.

Indeed, the length of esterifying alcohol clearly affects the spectral properties of the studied pigments, both in aqueous and non-polar environments. As neither naturally occurring esterifying alcohols nor the *n*-alcohols used in this study absorb in the visible-near infrared spectral region, the length of alcohol chain must cause the observed changes in absorption spectra indirectly. In fact, the length of the esterifying chain modifies the driving force of the aggregation that affects the excitonic coupling between the chlorin rings and thus determines the absorption spectrum.

In general (B)Chls are not well soluble in aqueous environment due to the hydrophobicity imposed by their esterifying alcohol. In contrast, BChl *c* is rather soluble in aqueous buffer, where the hydrophobic interaction between the farnesyl tails of BChl *c* drives them to form dimers (23). In this study, we have used X-BChlide *c* derivatives differing in the *n*-alkyl chain to prove with more detail that the hydrophobic driving force depends on the length of these moieties and that excitonic coupling in aqueous buffer is not evident until certain length of the *n*-alkyl chain is reached. Whereas Me-BChlide *c* remains in a monomeric form, because it is very polar and so freely dispersed in water, Do-BChlide *c* shows spectral features very similar to BChl *c* dimers, suggesting that the hydrophobic interaction between the *n*-dodecyl chains put the polar chlorins close enough to induce exciton interactions between the molecules. In general, the spectra of all X-BChlides in aqueous buffer can be described as a mixture of monomers and dimers. The formation rate and amount of dimers increases with esterifying alcohol length as a result of increasing hydrophobicity of the X-BChlide. This clearly shows that the hydrophobic effect is indeed the driving force for the dimer formation in polar environment. Interestingly, variations in the initial concentration of injected BChl *c* or X-BChlide *c* derivatives only lead to changes in the rate of dimer

Deleted: 2

formation, but not to the formation of higher aggregates with absorption maxima beyond 715 nm. This result contrasts with the autocatalytic aggregation of X-BChlide *c* in non-polar solvents as hexane (see below) and suggests that in aqueous buffer the formation of critical concentration of X-BChlide *c* cannot be reached to induce further aggregation. To induce formation of higher-state aggregates (absorption maxima around 740 nm) in aqueous environment, it is necessary to increase the hydrophobic interaction using lipids or carotenoids. In this work we observed that when MGDG is used, all X-BChlides form aggregates in a similar way showing that the lipid itself induces sufficient hydrophobic interaction. However, MGDG did not induce more extensive red shift for the aggregates from X-BChlide *c* with shorter esterifying alcohols, as reported in aqueous Triton X-100 solutions (30). Hydrophobic interactions between the long alkyl group of X-BChlide *c* derivatives and Triton X-100 molecules have also been suggested to stabilize X-BChlide *c* aggregates (36).

In non-polar environments we can expect that the driving force will be the hydrophilic interaction between polar chlorin rings. Indeed, we observed that the aggregation for Me-BChlide is fastest and most efficient; an opposite situation to that in aqueous environment. As BChl *c* is known to form aggregates in hexane, it is not surprising that aggregates were also developed by all the other X-BChlides with shorter alcohols. They all gave a similar Q_y peak position, in agreement with results reported for Me-BChl *c* and hexyl-BChl *c* (30). However, it is worth noting that the length of the esterifying alcohol again modifies the aggregation rate, this time in opposite direction to that in aqueous buffer. The slower aggregation of X-BChlide with longer *n*-alkyl chain is due to the stronger hydrophobic interaction between the *n*-alkyl chain and the hexane molecule. A detailed study of BChl *c* aggregation rates in non-polar solvents such as hexane has been reported in (40). The concentration dependence of BChl *c* self-

Deleted: 29

Deleted: 29

Deleted: alcohol

Formatted

Deleted: alcohol

Formatted

Deleted: 38

aggregation shows that the process undergoes autocatalysis, where formed aggregates catalyze further aggregation. The autocatalysis matches a sigmoidal type function with induction period dependent on the concentration of the injected BChl *c*. In our experiments, the final absorbance of BChl *c* self-aggregates in hexane was about 1 cm^{-1} at the Q_y band and matched the autocatalysis rate of few minutes reported for BChl *c* aggregates with similar absorbance as described in (38). Although we did not measure quantitatively the aggregate rate formation in this work, it was clear that the autocatalysis rate of Me-BChlide *c* is by far quicker than that of BChl *c* at similar concentrations (Fig. 4, inset). This trend is in agreement with results reported by (45), where the autocatalysis rate of Zn methyl bacteriopheophorbide *d* in aqueous tetrahydrofuran solution was determined to be in a subsecond time scale. The length of the esterifying alcohol thus modifies critical aggregation concentration required for the growing of aggregates via the solvation/resolvation exchange of the *n*-alkyl chain by hexane.

Deleted: 3

The role of the esterifying alcohol in the autocatalysis rate is manifested also when, instead of changing the length of the *n*-alkyl chain, *n*-alkanes with different carbon skeleton length (longer than hexane) are used as solvents. The hydrophobic interaction between farnesyl of BChl *c* and the *n*-alkane increases with the length of the solvent molecule and competes with the interaction between farnesyl chains themselves, thus slowing down the aggregation and increasing the amount of monomers and dimers in longer alkanes. It is worth mentioning that the viscosity, which increases with the length of the *n*-alkane (i.e. the viscosity coefficient goes from $3.3\ 10^{-5}$ Pa s for hexane to $2.2\ 10^{-4}$ Pa s for tetradecane), might be another factor slowering the aggregation. Due to slower aggregate development in longer *n*-alkanes, it could be clearly observed that the dimers are formed first and later converted into higher-state aggregates.

Previously, no significant changes were observed in the spectral properties of chlorosomes of *Chlorobium tepidum* and *Chloroflexus aurantiacus* when the esterifying alcohols were altered by growing bacteria in culture media supplemented with long (C_{10}-C_{20}) alcohols (34,35). These observations do not contradict the results we present in this study. The extent of the observed spectral changes in our study depends on the polarity of both X BChlide and the used solvent. The change of polarity is most significant going from MeOH to octanol as the esterifying alcohol, while the alcohols used in the previous studies (34,35) have a polarity similar to that of naturally occurring esterifying alcohols.

Deleted: 3
Deleted: 4
Deleted: 3
Deleted: 4

In summary, the results show that aggregation of chlorosomal BChls is controlled by both hydrophilic and hydrophobic forces, the latter mainly determined by the length of the esterifying alcohol. As a result, the properties of the BChl aggregate can be modified to some extent by the length of the esterifying alcohol. The results also suggest that the methyl substituents and the double bonds in the skeleton of farnesyl improve the aggregation of BChl *c*.

Acknowledgements--This research was supported by Czech Ministry of Education, Youth and Sports (projects MSM0021620835, MSM6007665808 and AV0Z50510513), Czech Science Foundation (project 206/05/2739), Spanish Ministry of Education and Science (project BF2004-04914-C02-02/BMC) and AVCR-CSIC joint project (projects 2004CZ0001 and 2006CZ0019). Authors would like to thank Frantisek Matousek and Ivana Hunalova for technical assistance.

REFERENCES

1. Blankenship R. E. and K. Matsuura (2003) Antenna complexes from green photosynthetic bacteria. In *Light-harvesting antennas*. (Edited by B. R. Green and W. W. Parson), pp. 195-217. Kluwer Academic Publishers, Dordrecht

2. Balaban, T. S., H. Tamiaki and A. R. Holzwarth (2005) Chlorins programmed for self-assembly. *Top. Curr. Chem.* **258**, 1-38.

3. Hildebrandt, P., H. Tamiaki, A. R. Holzwarth and K. Schaffner (1994) Resonance Raman-spectroscopic study of metallochlorin aggregates. Implications for the supramolecular structure in chlorosomal BChl *c* antennae of green bacteria. *J. Phys. Chem.* **98**, 2192-2197.

4. Balaban, T. S. (2005) Tailoring porphyrins and chlorins for self-assembly in biomimetic artificial antenna systems. *Acc. Chem. Res.* **38**, 612-623.

5. Holzwarth, A. R. and K. Schaffner (1994) On the structure of bacteriochlorophyll molecular aggregates in the chlorosomes of green bacteria. A molecular modelling study. *Photosynth. Res.* **41**, 225-233.

6. Balaban, T. S., A. R. Holzwarth, K. Schaffner, G. J. Boender and H. J. M. de Groot (1995) CP-MAS 13C-NMR dipolar correlation spectroscopy of 13C-enriched chlorosomes and isolated bacteriochlorophyll *c* aggregates of *Chlorobium tepidum*: The self organization of pigments is the main structural feature of chlorosomes. *Biochemistry* **34**, 15259-15266.

7. Chiefari, J., K. Griebenow, F. Fages, N. Griebenow, T. S. Balaban, A. R. Holzwarth and K. Schaffner (1995) Models for the pigment organization in the chlorosomes of photosynthetic bacteria: Diastereoselective control of *in vivo* bacteriochlorophyll c_s aggregation. *J. Phys. Chem.* **99**, 1357-1365.

8. van Rossum, B. J., D. B. Steensgaard, F. M. Mulder, G. J. Boender, K. Schaffner, A. R. Holzwarth and H. J. M. de Groot (2001) A refined model of the chlorosomal antennae of the green bacterium *Chlorobium tepidum* from proton chemical shift constraints obtained with high-field 2-D and 3-D MAS NMR dipolar correlation spectroscopy. *Biochemistry* **40**, 1587-1595.

9. Smith, K. M., F. W. Bobe, D. A. Goff and R. J. Abraham (1986) NMR spectra of porphyrins. 28. Detailed solution structure of bacteriochlorophyllide *d* dimer. *J. Am. Chem. Soc.* **108**, 1111-1120.

10. Nozawa, T., K. Ohtomo, M. Suzuki, H. Nakagawa, Y. Shikama, H. Konami and Z. Y. Wang (1994) Structures of chlorosomes and aggregated BChl *c* in *Chlorobium tepidum* from solid state high resolution CP/MAS 13C NMR. *Photosynth. Res.* **41**, 211-223.

11. Umetsu, M., Z. Y. Wang, J. Zhang, T. Ishii, K. Uehara, Y. Inoko, M. Kobayashi and T. Nozawa (1999) How the formation process influences the structure of BChl *c* aggregates. *Photosynth. Res.* **60**, 229-239.

12. Wang, Z. Y., M. Umetsu, M. Kobayashi and T. Nozawa (1999) Complete assignment of H1 NMR spectra and structural analysis of intact bacteriochlorophyll *c* dimer in solution. *J. Phys. Chem. B* **103**, 3742-3753.

13. Umetsu, M., R. Seki, Z. Y. Wang, I. Kumagai and T. Nozawa (2002) Circular and magnetic circular dichroism studies of bacteriochlorophyll *c* aggregates: T-shaped and antiparallel dimers. *J. Phys. Chem. B* **106**, 3987-3995.

14. Egawa, A., T. Fujiwara, T. Mizoguchi, Y. Kakitani, Y. Koyama Y. and H. Akutsu (2007) Structure of the light-harvesting bacteriochlorophyll *c* assembly in chlorosomes from *Chlorobium limicola* determined by solid-state NMR. *Proc. Natl. Acad. Sci.* **104**, 790-795

15. Staehelin, L. A., J. R. Golecki, R. C. Fuller and G. Drews (1978) Visualization of the supramolecular architecture of chlorosome (Chlorobium type vesicles) in freeze-fractured cells of *Chloroflexus aurantiacus*. *Arch. Microbiol.* **119**, 269-277

16. Staehelin, L. A., J. R. Golecki and G. Drews (1980) Supramolecular organization of chlorosome (Chlorobium vesicles) and of their membrane attachment site in *Chlorobium limicola*. *Biochim. Biophys. Acta* **589**, 30-45.

17. Psencik, J., T. P. Ikonen, P. Laurinmäki, M. C. Merckel, S. J. Butcher, R. E. Serimaa and R. Tuma (2004) Lamellar organization of pigments in chlorosomes, the light harvesting complexes of green photosynthetic bacteria. *Biophys. J.* **87**, 1165-1172

18. Psencik, J., J. B. Arellano, T. P. Ikonen, C. M. Borrego, P. A. Laurinmaki, S. J. Butcher, R. E. Serimaa and R. Tuma (2006) Internal structure of chlorosomes from brown-colored *Chlorobium* species and the role of carotenoids in their assembly. *Biophys. J.* **91**, 1433-1440.

19. Oostergetel, G. T., M. Reus, A. Gomez Maqueo Chew, D. A. Bryant, E. J. Boekema and A. R. Holzwarth (2007) Long-range organization of bacteriochlorophyll in chlorosomes of *Chlorobium tepidum* investigated by cryo-electron microscopy. FEBS. Lett. **581**, 5435-5439.

20. Bystrova, M. I., I. N. Mal'gosheva and A. A. Krasnovsky (1979) Study of molecular mechanism of self-assembly of aggregated forms of bacteriochlorophyll *c*. *Mol. Biol.* **13**, 440-451.

21. Smith, K. M., L. A. Kehres and J. Fajer (1983) Aggregation of the bacteriochlorophylls *c*, *d* and *e*. Models for the antenna chlorophylls of green and brown photosynthetic bacteria. *J. Am. Chem. Soc.* **105**, 1387-1389.

Formatted

Formatted

Deleted: 19

Deleted: 0

22. Hirota, M., T. Moriyama, K. Shimada, M. Miller, J. M. Olson and K. Matsuura (1992) High degree of organization of bacteriochlorophyll *c* in chlorosome-like aggregates spontaneously assembled in aqueous solution. *Biochim. Biophys. Acta* **1099**, 271-274.

23. Klinger, P., J. B. Arellano, F. E. Vacha, J. Hala and J. Psencik (2004) Effect of carotenoids and monogalactosyl diglyceride on bacteriochlorophyll *c* aggregates in aqueous buffer: Implications for the self-assembly of chlorosomes. *Photochem. Photobiol.* **80**, 572-578.

24. Kunieda, M. and H. Tamiaki (2006) Self-aggregation of synthetic zinc chlorins possessing a 13-ester-carbonyl group as chlorosomal chlorophyll models. *Eur. J. Org. Chem.* **10**, 2352-2361.

25. Mizoguchi, T., A. Shoji, M. Kunieda, H. Miyashita, T. Tsuchiya, M. Mimuro and H. Tamiaki (2006) Stereochemical determination of chlorophyll-*d* molecule from *Acaryochloris marina* and its modification to a self-aggregative chlorophyll as a model of green photosynthetic bacterial antennae. *Photochem. Photobiol. Sci.* **5**, 291-299

26. Balaban M. C. and T. S. Balaban (2007) Extending the self-organization algorithm of chlorosomal bacteriochlorophylls to synthetic pigments. *J. Porphyr. Phthalocya.* **11**, 277-286

27. Blankenship R. E., J. M. Olson and M. Miller (1995) Antenna complexes from green photosynthetic bacteria. In *Anoxygenic photosynthetic bacteria*. (Edited by R. E. Blankenship, M. T. Madigan and C. E. Bauer), pp. 399-435. Kluwer Academic Publisher, Dordrecht

28. Tamiaki, H. (1996) Supramolecular structure in extramembraneous antennae of green photosynthetic bacteria. *Coord. Chem. Rev.* **148**, 183-197.

Deleted: 1

Deleted: 2

Deleted: 3

Deleted: 4

Deleted: 5

Deleted: 6

Deleted: 7

29. Miyatake, T. and H. Tamiaki (2005) Self-aggregates of bacteriochlorophylls-*c*, *d* and *e* in a light-harvesting antenna system of green photosynthetic bacteria: Effect of stereochemistry at the chiral 3-(1-hydroxyethyl) group on the supramolecular arrangement of chlorophyllous pigments. *J. Photochem. Photobiol. C* **6**, 89-107.

30. Tamiaki, H., R. Shibata and T. Mizoguchi T (2007) The 17-propionate function of (bacterio)chlorophylls: Biological implication of their long esterifying chains in photosynthetic systems. *Photochem. Photobiol.* **83**, 152-162.

31. McDermott, G., S. M. Prince, A. A. Freer, A. M. Hawthornthwaite-Lawless, M. Z. Papiz, R. J. Cogdell and N. W. Isaacs (1995) Crystal-structure of an integral membrane light-harvesting complex from photosynthetic bacteria. *Nature* **374**, 517-521.

32. Hofmann, E., P. M. Wrench, F. P. Sharpless, R. G. Hiller, W. Welte and K. Diederichs (1996) Structural basis of light harvesting by carotenoids: Peridinin-chlorophyll-protein from *Amphidinium carterae*. *Science* **272**, 1788-1791.

33. Liu, Z., H. Yan, K. Wang, T. Kuang, J. Zhang, L. Gui and X. C. W. An (2004) Crystal structure of spinach major light-harvesting complex at 2.72 Å resolution. *Nature* **428**, 287-292.

34. Larsen K. L., M. Miller and R. P. Cox (1995) Incorporation of exogenous long-chain alcohols into bacteriochlorophyll *c* homologs by *Chloroflexus aurantiacus*. *Arch. Microbiol.* **163**, 119-123.

35. Steensgaard, D. B., R. P. Cox and M. Miller (1996) Manipulation of the bacteriochlorophyll *c* homolog distribution in the green sulfur bacterium *Chlorobium tepidum*. *Photosynth. Res.* **48**, 385-393.

Deleted: 8

Deleted: 29

Deleted: 30

Deleted: 2007

Deleted: 1

Deleted: 2

Deleted: 3

Deleted: 4

36. Mizoguchi, T. and H. Tamiaki (2007) The effect of esterifying chains at the 17-propionate of bacteriochlorophylls-*c* on their self-assembly. Bull. Chem. Soc. Jpn. **80**, 2196-2202.

37. Wahlund, T. M., C. R. Woese, R. W. Castenholz and M. T. Madigan (1991) A thermophilic green sulfur bacterium from New Zealand hot-springs, *Chlorobium tepidum* sp. nov. *Arch. Microbiol.* **156**, 81-90.

38. Borrego, C. M., P. D. Gerola, M. Miller, R. P. Cox (1999) Light intensity effects on pigment composition and organisation in the green sulfur bacterium *Chlorobium tepidum*. *Photosynth. Res.* **59**, 159-166.

39. Umetsu, M., R. Seki, T. Kadota, Z. Y. Wang, T. Adschiri and T. Nozawa (2003) Dynamic exchange properties of the antiparallel bacteriochlorophyll *c* dimers. *J. Phys. Chem. B* **107**, 9876-9882.

40. Balaban, T. S., J. Leitich, A. R. Holzwarth and K. Schaffner (2000) Autocatalyzed self-aggregation of (3(1)R)-[Et,Et]Bacteriochlorophyll *c*(F) molecules in nonpolar solvents. Analysis of the kinetics. *J. Phys. Chem. B* **104**, 1362-1372.

41. Steensgaard, D. B., H. Wackerbarth, P. Hildebrandt and A. R. Holzwarth (2000) Diastereoselective control of bacteriochlorophyll *e* aggregation. 3(1)-S-BChl e is essential for the formation of chlorosome-like aggregates. *J. Phys. Chem. B* **104**, 10379-10386.

42. Balaban, T. S., M. Linke-Schaetzel, A. D. Bhise, N. Vanthuyne, C. Roussel, C. E. Anson, G. Buth, A. Eichhofer, K. Foster, G. Garab, H. Gliemann, R. Goddard, T. Javorfi, A. K. Powell, H. Rosner and T. Schimmel (2005) Structural characterization of artificial self-assembling porphyrins that mimic the natural chlorosomal bacteriochlorophylls *c*, *d*, and *e*. *Chem. Eur. J.* **11**, 2268-2275.

Formatted

Formatted

Deleted: 5

Deleted: 6

Deleted: 7

Deleted: 38

Deleted: 39

Deleted: 0

43. Uehara, K., M. Mimuro, Y. Ozaki and J. M. Olson (1994) The formation and characterization of the in-vitro polymeric aggregates of bacteriochlorophyll *c* homologs from *Chlorobium limicola* in aqueous suspension in the presence of monogalactosyl diglyceride. *Photosynth. Res.* **41**, 235-243.

44. Mizoguchi, T., K. Hara, H. Nagae and Y. Koyama (2000) Structural transformation among the aggregate forms of bacteriochlorophyll *c* as determined by electronic-absorption and NMR spectroscopies: Dependence on the stereoisomeric configuration and on the bulkiness of the 8-C side chain. *Photochem. Photobiol.* **71**, 596-609.

45. Miyatake, T., K. Shitasue, Y. Omori, K. Nakagawa, M. Fujiwara, T. Matsushita and H. Tamiaki (2005) Time-dependent self-assembly of 3(1)-epimerically pure and mixed zinc methyl bacteriopheophorbides-*d* in an aqueous THF solution. *Photosynth. Res.* **86**, 131-136.

Deleted: 1

Deleted: 2

Deleted: 3

FIGURE LEGENDS

Figure 1. HPLC chromatograms of X-BChlide *c* derivatives and BChl *c*: (a) H-BChlide *c*, (b) Farnesyl-esterified BChl *c* used for chemical transesterification reactions, (c) Me-BChlide *c*, (d) Bu-BChlide *c*, (e) Oc-BChlide *c*, (f) Do-BChlide *c*. For (c)–(e), KOH concentration was <0.1% and the rectangle shows the remaining BChl *c* under the assayed conditions. For (f), Me-BChlide *c* is the starting substrate for transesterification (<0.1% KOH). Detection wavelength is 430 nm. Other HPLC conditions are described in material and methods.

Figure 2. Absorption spectra of X-BChlide *c* derivatives and BChl *c* in aqueous buffer after 24 h of incubation: (a) Me-BChlide *c*, (b) Bu-BChlide *c*, (c) Oc-BChlide *c*, (d) Do-BChlide *c* and (e) BChl *c*. The inset shows the initial absorption spectra of Me-BChlide *c* (a) and Do-BChlide *c* (d) 5 min after preparation.

Figure 3. Absorption spectra of X-BChlide *c* derivatives and BChl *c* in hexane after 4 h of incubation: (a) Me-BChlide *c*, (b) Bu-BChlide *c*, (c) Oc-BChlide *c*, (d) Do-BChlide *c* and (e) BChl *c*. The rectangle highlights the spectral region with the most pronounced differences between the samples. The inset shows the initial absorption spectra of Me-BChlide *c* (a) and Do-BChlide *c* (d) 5 min after preparation.

Figure 4. Absorption spectra of BChl *c* in *n*-alkanes after 24 h of incubation: (a) hexane, (b) octane, (c) decane, (d) dodecane and (e) tetradecane. Inset shows absorption spectra of BChl *c* in hexane (a) and tetradecane (e) 15 min after preparation.

Figure 5. Absorption spectra of BChl *c* in decane. Spectra were measured at 0, 10, 30 min and 4, 24 and 48 h after preparation.

TABLE

Table 1. Experimental and theoretical (in brackets) values of the molecular masses for the four main homologues of the used X-BChlides. The molecular masses were rounded to the first decimal place.

	Me-BChl *c*	**Bu-BChl *c***	**Oc-BChl *c***	**Do-BChl *c***	**BChl *c***
[E,M]	n.d. (603.0)	n.d. (645.1)	n.d. (701.2)	n.d. (757.3)	792.8 (793.3)
[E,E]	616.7 (617.0)	659.0 (659.1)	714.9 (715.2)	770.5 (771.3)	806.6 (807.4)
[P,E]	630.4 (631.1)	672.6 (673.1)	728.6 (729.2)	784.5 (785.4)	820.6 (821.4)
[I,E]	n.d. (645.1)	n.d. (687.2)	742.3 (743.3)	n.d. (799.4)	834.3 (835.4)

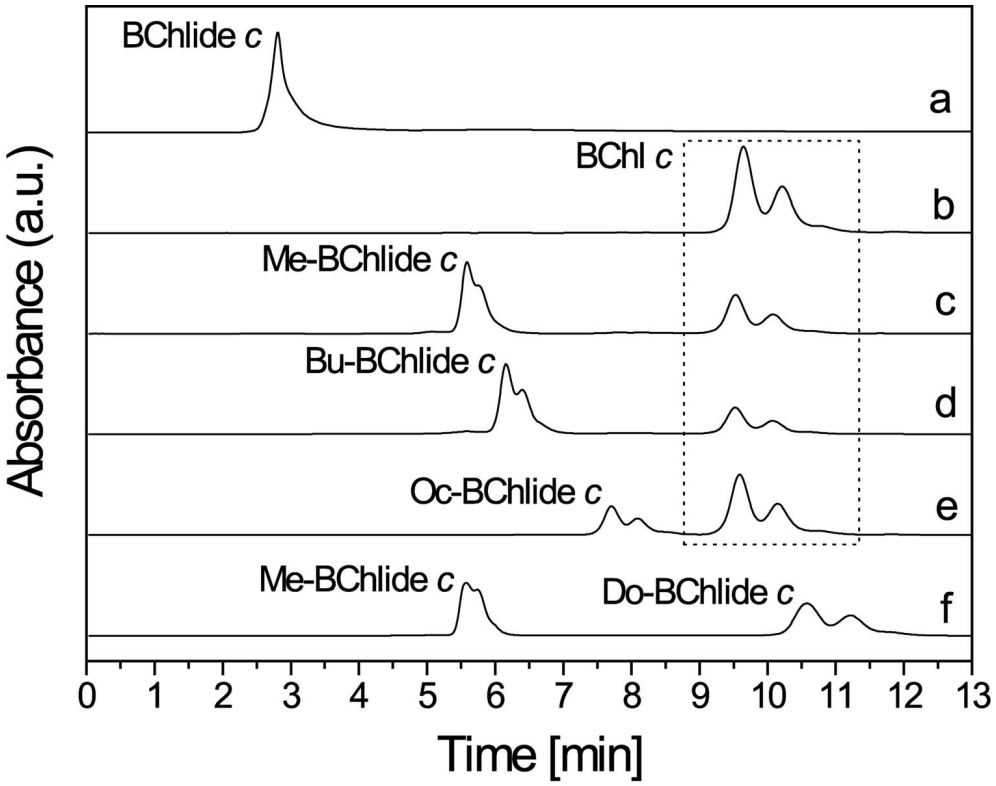

65x50mm (600 x 600 DPI)

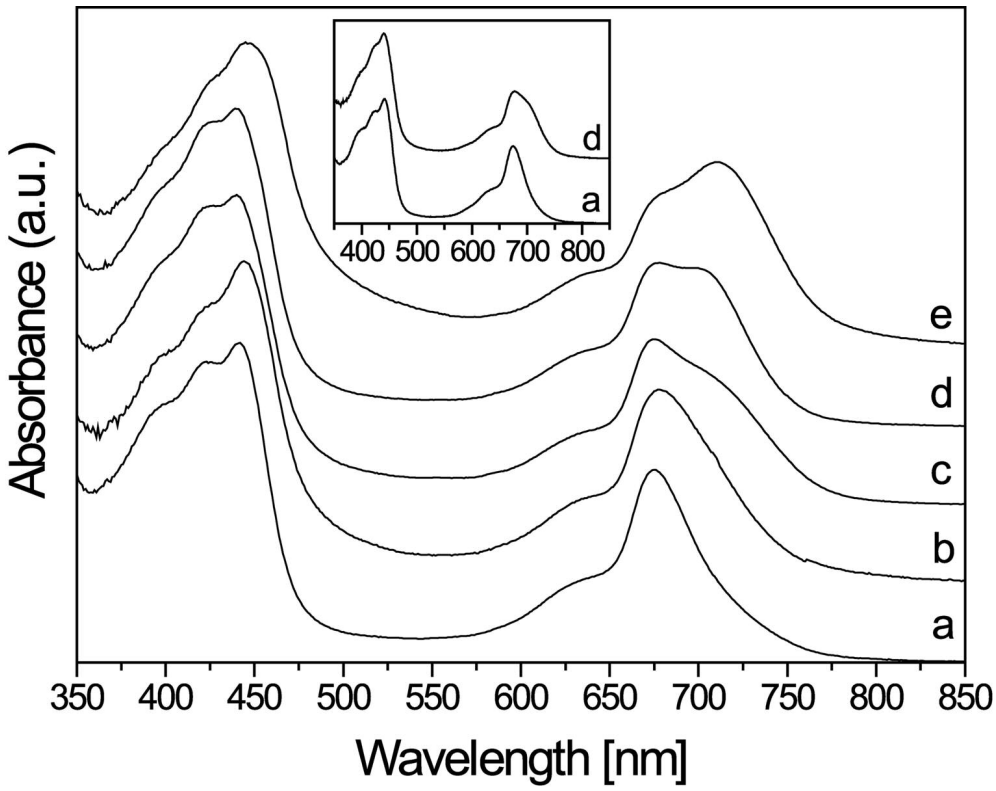

65x51mm (600 x 600 DPI)

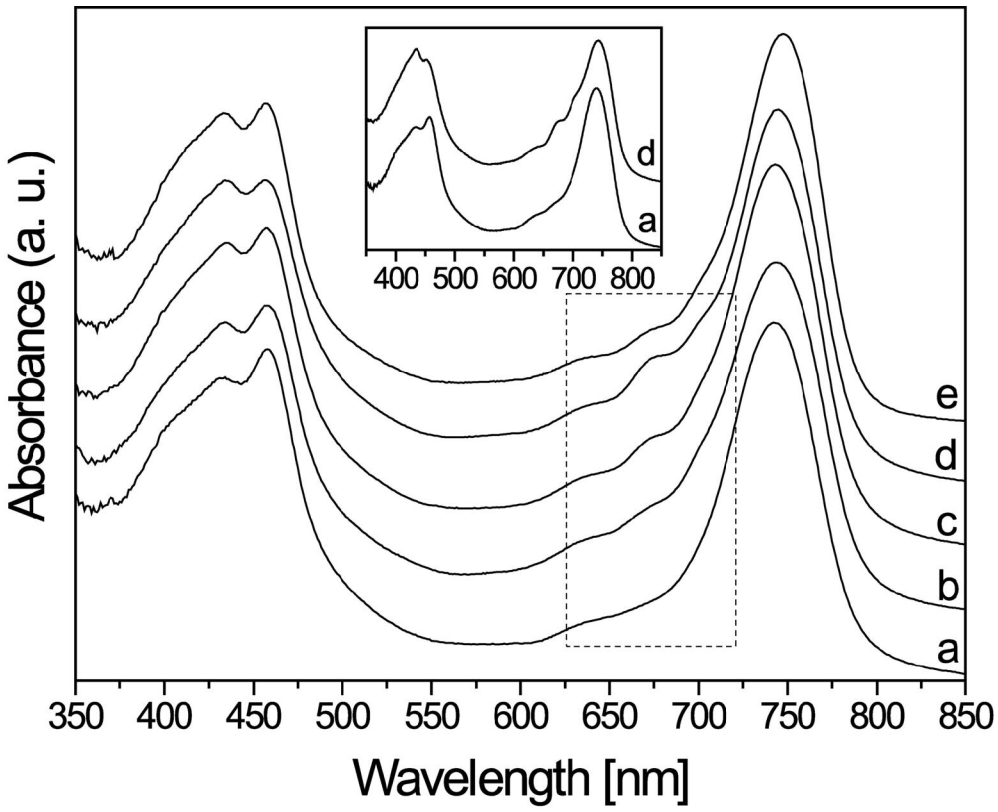

66x53mm (600 x 600 DPI)

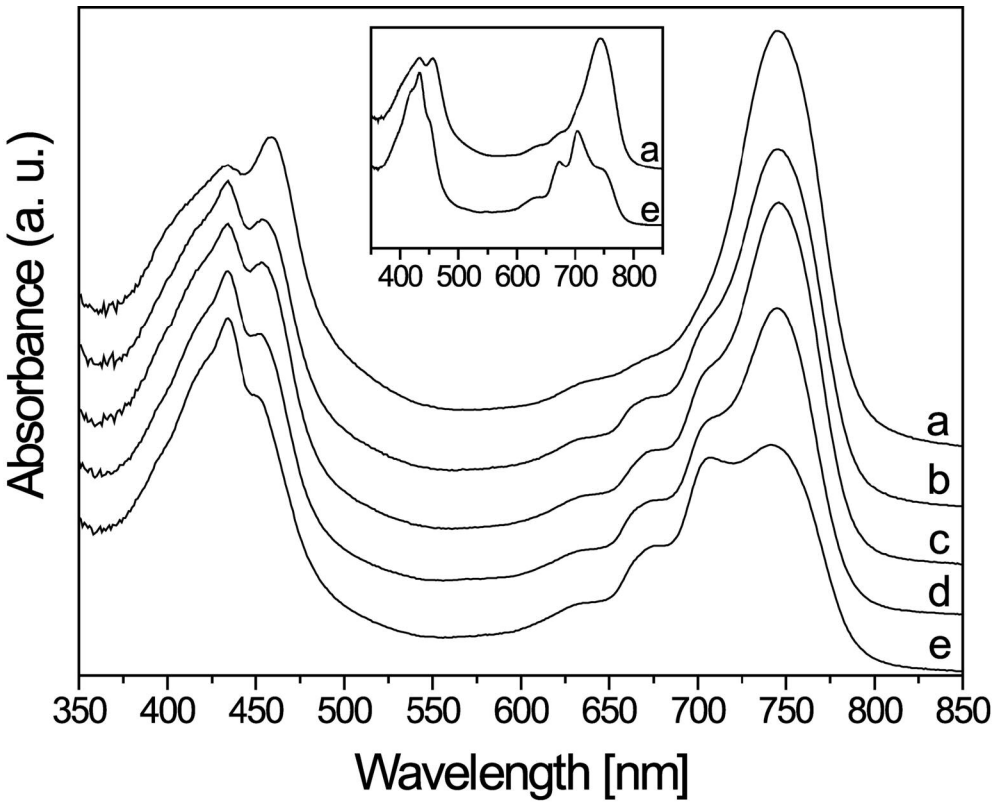

66x52mm (600 x 600 DPI)

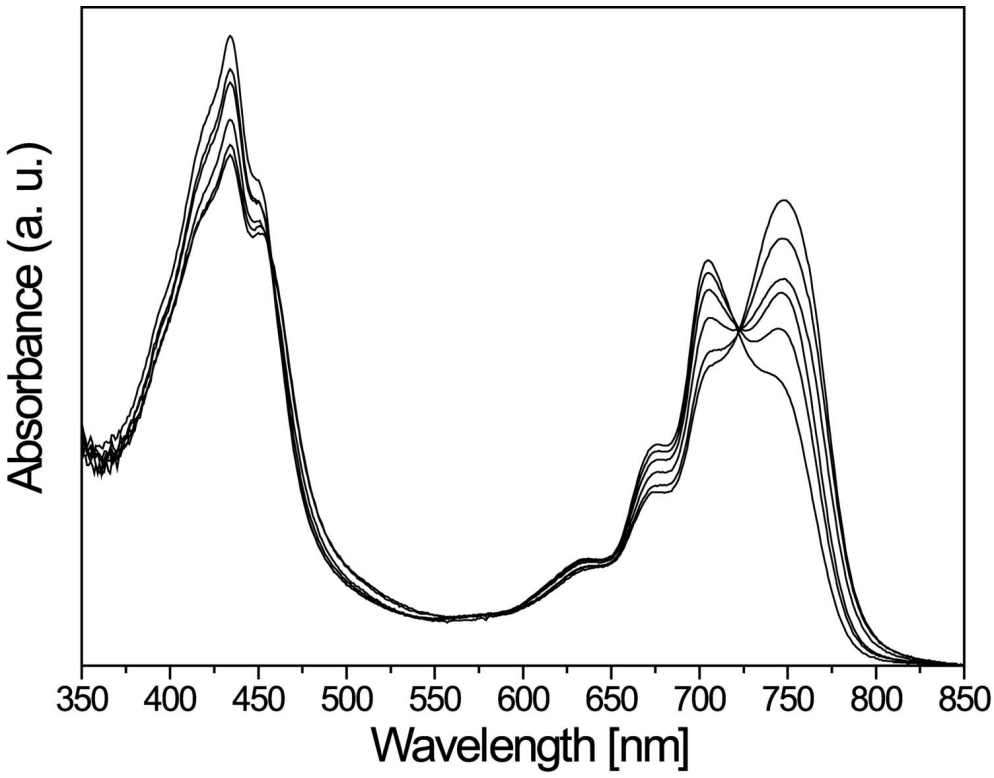

63x49mm (600 x 600 DPI)